International Journal of Automotive and Mechanical Engineering
ISSN: 2229-8649 (Print); ISSN: 2180-1606 (Online)
Volume 15, Issue 4 pp. 5914-5926 Dec 2018

Optimisation of Current and Pulse Duration in Electric Discharge Drilling of D2 Steel Using Graphite Electrode

D. Deepak[1*], P. Shrinivas[1], G. Hemant[1] and R. Iasy[2]

[1]Department of Mechanical and Manufacturing Engineering,
Manipal Institute of Technology, Manipal Academy of Higher Education,
Manipal-576104, India
[*]Email: deepak.d@manipal.edu
[2]Mechanical Engineering Department, Ecole Polytechnique,
Federal De Lausanne 1015 Lausanne, Switzerland

ABSTRACT

Electric discharge machining (EDM) is one of the viable techniques for machining of D2 steel, in which the material removal occurs by spark erosion. The poor selection of EDM parameters affect the machining quality and productivity. Considering this, the present work investigates the effect of current, charging and discharging time on the material removal rate (MRR) and the surface roughness (R_a) while machining of D2 steel using graphite electrode. The results were analysed using statistical methods to identify the effect of control parameters and to optimise the settings. The study shows that MRR and R_a was significantly influenced by current. At optimum settings, the MRR and the R_a obtained was 38.16 mg/min and 3.39 µm respectively. Morphological analysis of the machined surface show that the size of the globules formed decreased with increase in current.

Keywords: Electric discharge drilling, graphite electrode, globules, material removal rate, surface roughness

INTRODUCTION

In the recent era, EDM has drawn great attention among the researchers due to its wide range of industrial applications. The process is capable of machining extremely hard and tough materials with relatively softer tools like copper, aluminium, graphite, etc. The material removal occurs primarily by spark erosion i.e., melting and vaporization of the workpiece. A closely spaced electrically conductive tool and a workpiece, submerged in dielectric medium generate the discrete sparks which result in vaporizing a portion of material from the workpiece. A small volume of material removal also occurs on the tool surface. This process is capable of machining intricate cavities, contours with good surface finish and dimensional accuracy. The major limitations of the process are low MRR and requirement of electrical conductivity in the tool and the workpiece. Generally, materials like hardened steel, tool steel, carbide, inconel, titanium, and other alloys are machined using EDM. For manufacturing of automotive, aircraft and machine tool components, D2 tool steel is extensively used due to their superior strength, wear resistance and high thermal stability. Machining of such materials by traditional methods generate intense heat due to high shear and friction at the interface of tool and work material [1]. The high temperature in the cutting zone affects the material properties of both cutting tool and workpiece. The softening of cutting tool due to high temperature

results in degradation of its cutting performance. In this scenario, non-traditional methods like EDM, abrasive water jet machining [2], laser beam machining etc., are found to be viable machining methods.

Vinothkumar and Pradeepkumar [3] investigated the effect of EDM control parameters like input current (Ip), gap voltage and pulse-on time (Ton) on MRR, electrode wear ratio (EWR) and surface roughness while machining of D2 steel using a non-cooled and a cryogenically cooled copper tool. When a non-cooled tool was used, the EWR and MRR significantly increased by 35.31 % and 59.22 % respectively for change in current from 9 A to 15 A. The surface roughness increased from 6.4 µm to 12.8 µm with increase in Ip and Ton (100 µs to 200 µs). The use of cryogenically cooled tool reduced the EWR by 10-21 % and Ra by 5-10 % compared to non-cooled tools. Pradhan and Biswas [4] investigated white layer thickness, surface crack density and Ra produced by the copper tool having positive polarity. The study show that surface integrity was significantly influenced by Ton (27.46 %), followed by duty factor (Tau - 23.87 %) and Ip (18.46 %). Nayak et al [5] studied the effect of Ip, Tau and Ton on MRR, Ra, crack density and residual stress using cylindrical copper tool. The percentage contribution of Ip was highest on MRR (95.65 %) and Ra (95.8%), whereas Ton and Tau showed marginal effect. The crack density on the machined surface was decreased with increase in Ip (57%) and Ton (34%). The optimum surface integrity was achieved at Ip-3 A, Ton-300 µs and Tau- 45%.

Electrical conductivity is the critical factor in selection of EDM tool material. Graphite tools are generally used for roughing operations due to low tool wear rate (TWR), good electrical and thermal properties. Klocke et al., [6] studied the effect of I_p and T_{on} on MRR and TWR using graphite tools having different electrical resistance, thermal conductivity and grain size. The MRR and TWR was significantly influenced by I_p and T_{on} respectively. But, the relationship between different grades of graphite, MRR and tool wear was not established. Al Hazza et al., [7] investigated the performance of Cu, Al and graphite tools on MRR and EWR while machining of AISI 304 stainless steel. Study showed that the MRR and EWR increased with increase in I_p irrespective of tool materials. Among the tooling materials, graphite tools exhibited lowest EWR and highest MRR. The use of flexible generator further increased the MRR by 50 % compared to conventional generators [8]. Klocke et al., [9] used metal infiltrated tools as an alternative for tungsten copper alloy and graphite tools for machining of cemented carbide. Although tungsten copper alloy tools are expensive, they showed good performance. Use of bronze infiltrated graphite resulted in reduction of tooling cost by about 24 % compared to copper tungsten alloy during rough cutting. Finishing process showed that bronze infiltrated graphite tools resulted in reducing the surface roughness by 12 %, white layer thickness by 1 µm and increased fracture toughness compared to machining by copper tungsten alloys.

Lee et al., [10] presented a detailed overview of challenges in real-time measurement of electrode wear, dependency on shape of holes and tool materials while drilling (by EDM) high strength steel, cemented carbide and titanium alloys. A semi empirical model was proposed by Izwan et al., [11] to predict the MRR of Al 6061-T6, Domex 550 MC steel, HSLA steel and brass alloy using a rotary copper electrode. The MRR was dependent on cumulative electrical charge obtained from individual sparking cycle and the highest MRR was obtained at higher I_p and a longer T_{on} duration. Sharif et al., [12] established models to relate I_p, V, T_{on} and T_{off} with MRR, TWR, R_a and dimensional accuracy while die-sinking of stainless steel (3161) using copper impregnated graphite tool. Deepak et al., [13] optimised the process parameters which

produced minimum R_a while EDM of D2 using copper tool and established constant value to predict the R_a. The study showed that current was the most significant factor which influenced the response. Kuppan et al., [14] evaluated the performance of copper and graphite electrodes (MRR, EWR and R_a) while deep drilling of holes (up to 25 mm depth with 3 mm diameter) on Inconel 718. The MRR and R_a was found to increase at different magnitude with increase in current (4 A to 10 A), irrespective of tool materials. At I_p-6 A, T_{au}-55 % and tool speed-200 rpm, the MRR was increased by 350 %, 150 %, 320 % and the R_a values were increased by 32 %, 30 %, 31 % for Cu, Cu-W and graphite tools respectively. Low EWR (<1 %) was achieved by graphite tools compared to Cu and Cu-W tools. Ablyaz et al., [15] investigated the tool wear for machining of structural steel using different types of tooling materials namely, copper, Cu coated Al alloy (AK12) and Al alloy (AK12) at settings I_p -3 A, T_{on}-50 µs, V-50 V, T_{au} -26 % for duration of 1 hour on constant machining area. Wear on Al was found to be 0.7 mm and for Cu and Cu coated tools wear was less than 0.1 mm. Al tool showed lower MRR (0.52 mm/h) compared to Cu (0.92 mm/h) and Cu coated tools (0.89 mm/hr). Study showed that coated electrodes with an inexpensive core resulted in good productivity and lesser tooling cost.

Özerkan [16] investigated MRR, TWR and R_a produced during EDM of Hadfield steel using a graphite tool at different I_p, T_{on}, T_{off} and polarity. For both negative and positive polarities, the TWR decreased and R_a increased with increase in current and T_{on}. Least TWR was obtained at maximum current of 50 A with reverse polarity. Machining by direct polarity produced higher MRR (25 %-81 %) compared to reverse polarity. He et al., [17] investigated die-sinking of 45# carbon steel using Cu-W electrodes. The effect of I_p, T_{on}, T_{au} and open circuit voltage were studied on TWR, electrode wear profile and the impact of carbon layer deposition on the electrode. Study showed that carbon layers were formed on the tool mainly due to migration of carbon from the dielectric fluid. The thickness of carbon layer was about 15 µm to 20 µm and its formation on the tool resulted in reduction of TWR.

The literature review of electric discharge machining of D2 steel show that there is a scope to establish the optimum process parameters which reduce the tooling time and machining cost of complex profiles. In consideration of this, the present work is carried out to determine the optimum machining parameters for drilling of D2 tool steel. Graphite electrodes are used due to ease of machining to give desired profile, good electrical conductivity and low wear rate compared to other metal electrodes. The study elucidates the effect of I_p, T_{on} and T_{off} on MRR and surface morphology. An attempt is also made to establish the relation between these parameters on the size of the globules formed on the drilled surface using image processing techniques.

METHODOLOGY

Experimental Setup

Methodology of the experimental work is shown in Figure 1 while Figure 2 shows the EDM (Make: VME, India and Model: V3525) used for experimental work. The dielectric fluid used for the machining is supplied by Carol Petroleum Pt. Ltd. India. The kinematic viscosity of fluid is 4-5 cSt (at 40 °C) and its flashpoint is 108°C. The flow rate of dielectric fluid is maintained constant during the experiments. The machine tool is equipped with a servo control mechanism with anti-arc control system. Detailed specification of machine is given in Table 1.

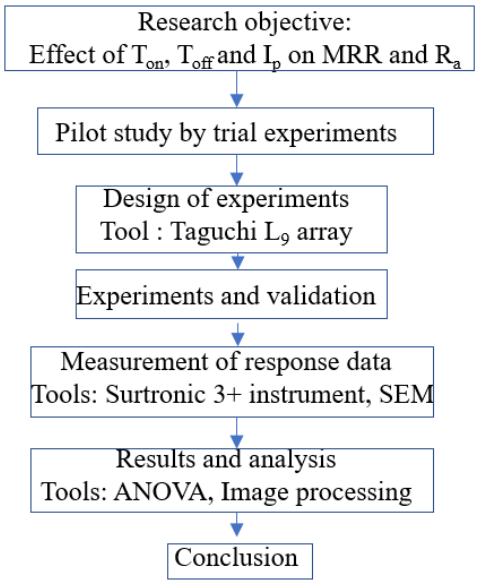

Figure 1. Experimental methodology

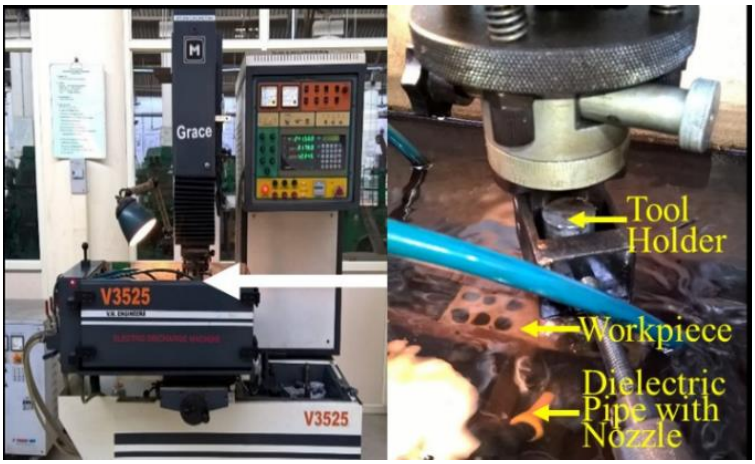

Figure 2. Experimental setup

Table 1. Machine specifications

Operating parameters	Specification
Input voltage	415 V AC, 50 Hz
Max. current	25 A
Max. open circuit voltage	75 V
Pulse ON/OFF settings	2 µs to 2000 µs
Vibrations	1 g, 10 Hz to 50 Hz
Table resolution	1 µm

Tool and Workpiece

Graphite electrodes (thermal conductivity of 70 W/m °C) of 10 mm diameter was used as tool. The approach surface of the tool is made flat by turning operation before the experiments. Each experiment is conducted with separate electrodes to account for

variation in machining characteristics due to electrode wear. The workpiece used is AISI D2 steel of thickness 4 mm. The hardness of the workpiece is 62 HRC and its modulus of elasticity is 207 GPa. Table 2 shows the chemical composition of the workpiece as obtained by elemental mapping method.

Table 2. Chemical composition of the workpiece (%)

C	Si	P	S	Cr	Mn	Fe	Co	Ni	Cu
1.6	0.4	0.03	0.03	13	0.40	82.76	0.99	0.37	0.37

Experimental Design

EDM process parameters are grouped into electrical, work and tool material and non-electrical parameters. Figure 3 shows the detailed list of EDM parameters influencing the TWR, MRR, kerf taper and R_a, etc. In the present work, properties of the work and tool materials are kept constant in all experiments. Influence of key electrical parameters like discharge current, spark on time and spark off time on response parameters are studied. The pulse on time is the time during which spark discharge occurs, while the pulse off time is the time between two spark discharges. Due to economic viability experiments are designed using Taguchi L_9 orthogonal array with three replications. The process parameters as well as their levels of the study are shown in Table 3 and the experimental design is shown in Table 4. The response data is analysed using analysis of variance (ANOVA) to identify the influence of various control parameters.

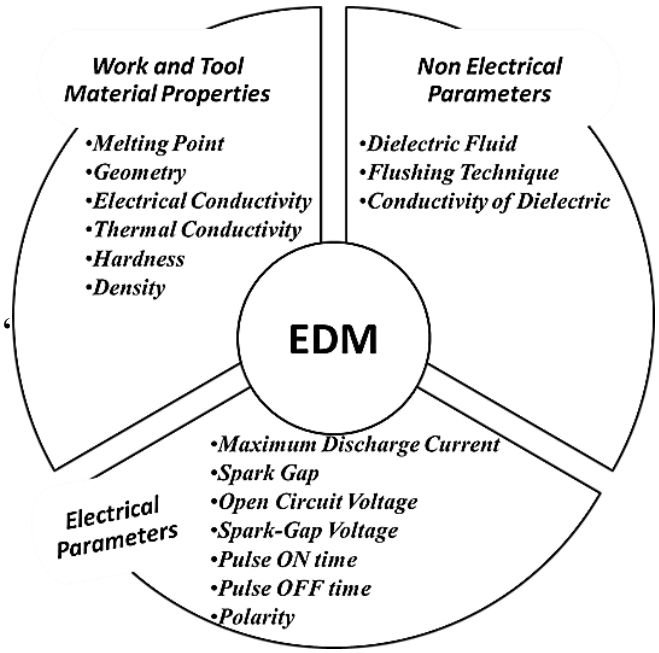

Figure 3. EDM process parameters.

Table 3 Process parameters and their levels.

Process Parameters	Code	Unit	Level 1	Level 2	Level 3
Current	I_p	A	6	7.5	9
Pulse on time	T_{on}	µs	5	20	100
Pulse off time	T_{off}	µs	100	500	2000

Table 4 Experimental design and average response data.

Exp. No.	I_p (A)	T_{on} (µs)	T_{off} (µs)	MRR (mg/min)	R_a (µm)
1	6	5	100	18.20	4.58
2	6	20	500	17.04	3.98
3	6	100	2000	12.71	8.86
4	7.5	5	100	35.08	3.76
5	7.5	20	500	16.15	6.86
6	7.5	100	2000	8.05	5.20
7	9	5	100	29.79	5.30
8	9	20	500	33.29	4.84
9	9	100	2000	22.30	7.44

Measurement of Response Parameters

The MRR is measured by weight *(W)* loss method over time (t) using Eq. (1). The surface roughness (R_a) of the hole was measured using Taylor Hobson surtronic 3+ instrument at five different locations. The specifications of surface measuring device are resolution - 0.01 µm, gauge range - 150 µm, stylus traverse speed - 1 mm/s, radius of diamond tipped stylus - 5 µm. The R_a value for known sampling length *(L)* on each drilled hole surface is calculated using the Eq. (2) [18]. Morphological study of the drilled hole surface is made by using scanning electron microscope (Model: EVO MA18).

$$MRR = \frac{W_i - W_f}{t} \text{ mg/min} \tag{1}$$

$$R_a = \frac{1}{L}\int_0^L Z(x)\,dx \ \mu m \tag{2}$$

Theoretical Models

The erosion modelling of the EDM is complex due to influence of various interdependent variables involved in the process. In EDM, the material removal occurs through electric discharge in the spark gap. The voltage (V) supplied between the electrode and workpiece, the corresponding spark energy developed is given by Eq. (3) and Eq. (4) [19] respectively. In addition to E_s, the material removal also depends on the spark frequency, f in Eq. (5), which is governed by charging and discharging time of the capacitor. The heat produced by the spark primarily depends on current, pulse time and voltage. Although, there are different models to predict the spark radius, the Gaussian heat input model is popularly used among the researchers [20-21]. According to this model, the maximum heat intensity is at the axis of a spark and the corresponding heat flux (q_f) is

given by Eq. (6) [22]. Where, W_m- energy utilized by the material, R- radial distance from the spark axis, r_{sp} - plasma channel radius, C- capacitance and R_c- resistance in the charging circuits.

$$V_{ct}=V\times(1-e^{(-t/CRc)}) \quad (3)$$

$$E_s=I_p\times V\times t_{on} \quad (4)$$

$$f=\frac{1}{t_{on}+t_{off}} \quad (5)$$

$$q_f(R)=\frac{4.45\times W_M\times I\times V}{\Pi\times(r_{sp})^2}\times e^{[-4.5(\frac{R}{r_{sp}})^2]} \quad (6)$$

RESULTS AND DISCUSSION

Effect of I_p, T_{on} and T_{off} on Material Removal Rate

The effect of I_p, T_{on} and T_{off} is shown in Figure 4. It is seen that, the MRR is increased almost linearly with increase in current. The spark energy (E_s) released by a single spark is directly proportional to input current which gets transformed into thermal energy. Hence, at higher input current, the intense thermal energy acting on the workpiece resulted in melting and vaporization of greater volume of material and increased the MRR with increase in current. Further, it is observed that increase in duration (T_{on}) of the current supplied in each pulse reduced the MRR almost linearly. Increase in T_{on}, reduced the spark frequency by 95%. The number of sparks produced at T_{on} of 5 µs, 20 µs and 100 µs (T_{off} at 100 µs, 500 µs, 2000 µs) are 9523, 1923 and 476 respectively. Due to decrease in sparks frequency, the corresponding thermal action on the workpiece is also greatly reduced, thus affecting the MRR. Interestingly, increase in spark delay time (T_{off}) from 100 µs to 500 µs resulted in improving the MRR by 24.8 %, but further increase (T_{off}: 2000 µs) resulted in decreasing the MRR. During T_{off} period, the dielectric fluid gets deionized and the debris were removed from the spark region by the flushing action of dielectric fluid. In addition, capacitor accumulated the sufficient current charge for the next discharge cycle which produced the sparks with great thermal energy. At shorter T_{off} the spark frequency is high, and its duration is almost 41.66 % of the pulse duration (T_{off} + T_{on}). Due to high spark frequency, the time available for flushing the debris out of machining zone is insufficient. Hence, small volume of vaporized metal is re-solidified in the form recast layer as shown in Figure 6(a).

Apart of the heat produced by successive sparks is transferred to the recast layer apart from melting the fresh work surface. Due to these factors low MRR is observed at short T_{off} (100 µs). Increase in T_{off} enhanced the flushing of debris which reduced the volume of debris welded on the work surface. Also, the capacitor is charged upto its critical charging range (0.63 *V*) during this period. Thus, the intense heat produced by these sparks at T_{off} -500 µs resulted in improving the MRR. Beyond the critical range, the charging of capacitor does not occur. Hence, longer T_{off} (2000 µs) increased the idle time of machining, i.e., the spark frequency and its duration (2.08 %) was decreased which resulted in reduction of MRR. Study shows that the spark duration of 8.33 % of the total pulse time is the optimum duration which produced maximum MRR. The contribution of

I_p, T_{on} and T_{off} on MRR is determined using ANOVA and is shown in Table 5. It shows that both T_{on} and I_p are the most influential process parameters compared to T_{off} which influenced the material removal rate.

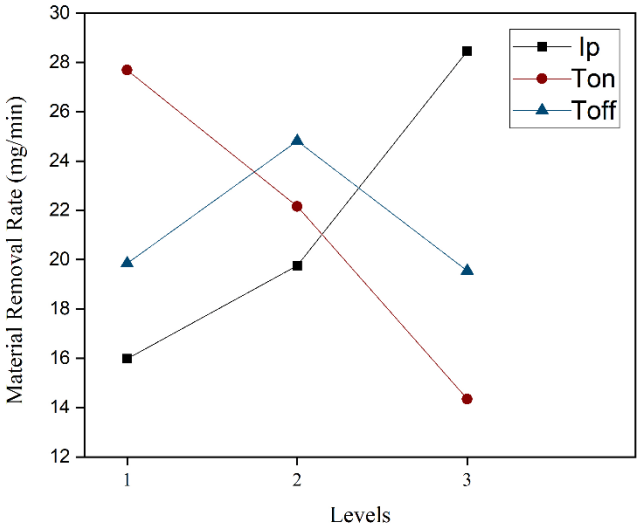

Figure 4. Main effect plot of material removal rate.

Table 5. ANOVA for material removal rate.

Source	DF	Sum of Square	Mean Square	F	% Contribution
I_p	2	245.46	122.73	1.72	43.28
T_{on}	2	269.31	134.66	1.88	47.50
T_{off}	2	52.29	26.15	0.37	9.22

Surface Roughness and Morphology

Figure 5 shows the effect of I_p, T_{on} and T_{off} on surface roughness. It shows that, increase in current from 6 A to 9 A, increased the surface roughness from 4.90 µm to 9.95 µm. According to Gaussian heat distribution model in Eq. (6), the maximum heat intensity lies on the axis of the spark. The spark radius and its intensity increased (Eq. 4) with increase in current which resulted in vaporization of material with deeper penetration and formation of craters as shown in Figure 6 (a) to (c). During deionization period of dielectric fluid, a part of the molten metal was flushed out of the craters re-solidified and resulted in formation of recast layer which resembled the wave patterns with peaks and valleys on the machined surface. The shape of the craters was enlarged with increase in current. During vaporization, the interaction between the dielectric fluid and the molten metal resulted in formation of smaller globules due to collapsing of vapours in the molten pool around the spark gap. Some of the globules were flushed away from the machined surface by the flood of dielectric fluid and a few of them was welded to the machined surface itself as shown in Figure 6 (a) to (d).

The enlarged view of the globules (debris) in a crater is shown in Figure 6(d). These factors led to increase surface roughness with increase in current. Further, the size of globule is estimated by digital processing of microscopic images and its distribution at different pulse duration and current is shown through Figure 7 (a) to (c). It is observed

that globules become finer (small sized globules) with increase in current due to intense vapour pressure developed in the spark gap at high current (9 A). The size of the globule produced is not significantly influenced by change in pulse duration. However, it is also seen from Figure 5 that increase in T_{on} led to marginal variation of surface roughness.

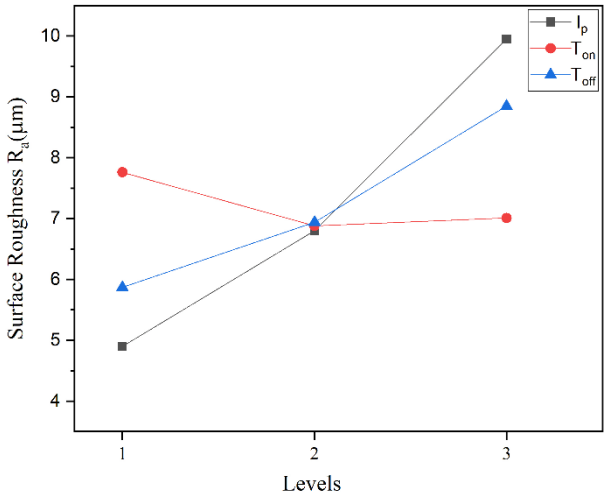

Figure 5 Main effect plot of surface roughness.

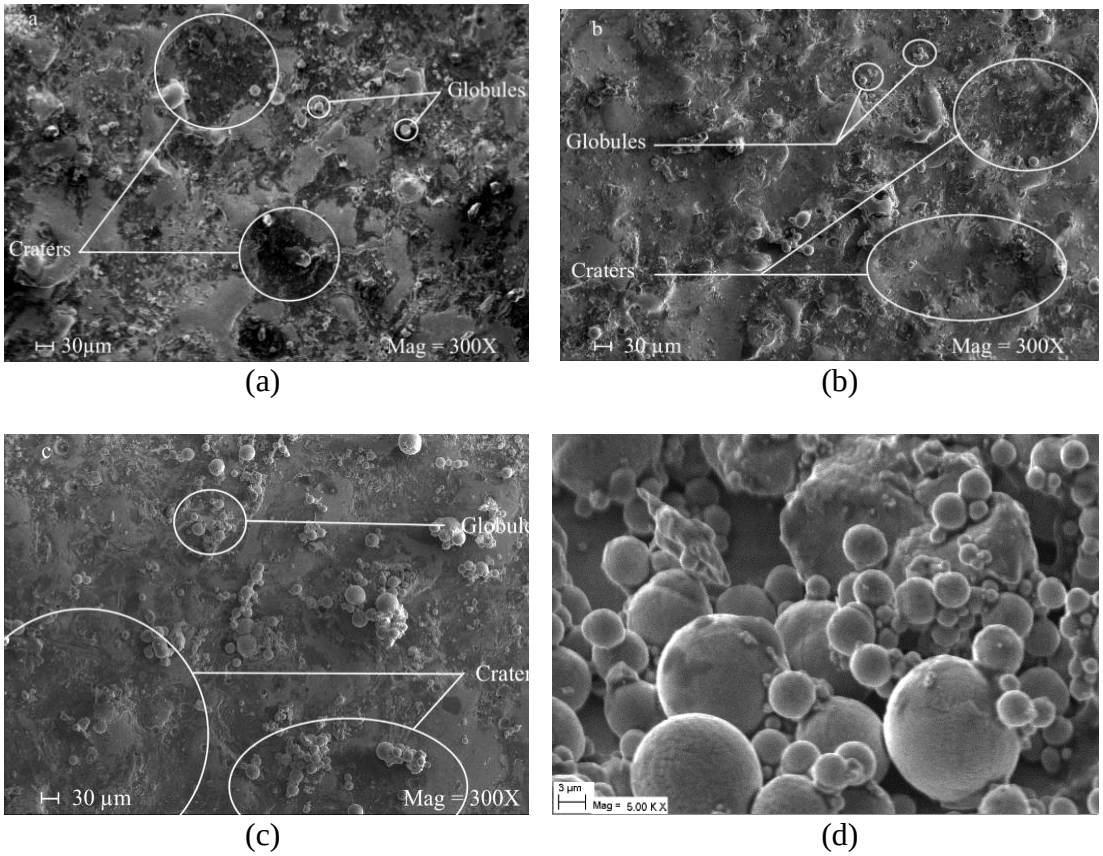

(a) (b)

(c) (d)

Figure 6. Machined surface at I_p of (a) 6 A (b) 7.5 A and; (c) 9 A. (d) A closer view of debris.

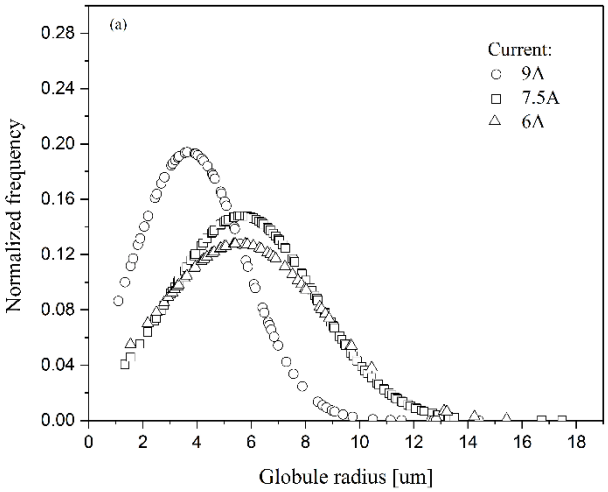

(a) pulse duration of 105 µs

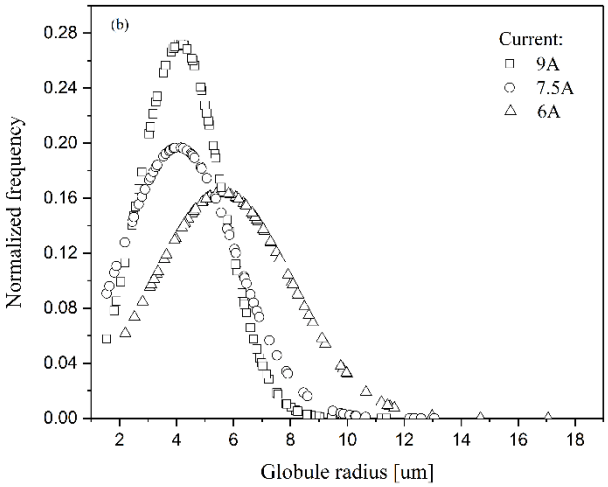

(b) pulse duration of 520 µs

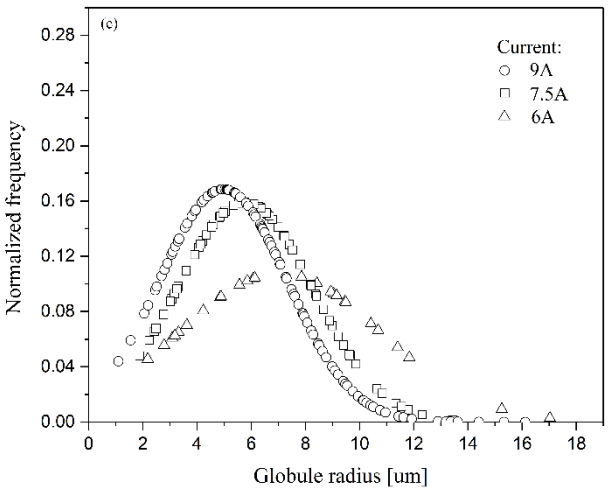

(c) pulse duration of 2100 µs

Figure 7. Size of globules at different pulse durations.

From ANOVA shown in Table 6, the effect of T_{on} is insignificant and its contribution on the surface roughness is 2.5%. But increase in T_{off} from 100 µs to 2000 µs increased the R_a from 5.87 µm to 8.85 µm. Increase in T_{off} decreased the spark frequency. Due to long duration between sparks, a portion of the molten metal experience the high compressive force exerted by the flow of dielectric fluid. This form uneven surface in the form of recast layer, hence increasing the surface roughness. The variance of response due to I_p, T_{on} and T_{off} is subjected to F test. It is seen that F values associated with I_p and T_{off} is higher than the $F_{critical}$ value. Hence, I_p and T_{off} are the most significant process parameters controlling the surface roughness. The influence of I_p is highest (71.72%) followed by T_{off} (25.08).

Table 6 ANOVA for surface roughness

Source	DF	Sum of square	Mean square	F	% Contribution
I_p	2	39.08	19.54	102.92	71.72
T_{on}	2	1.36	0.68	3.59	2.50
T_{off}	2	13.66	6.83	35.98	25.08

Optimisation of Process Parameters

The criterions for optimisation are, to improve the production rate by increasing MRR and reduce the surface roughness of machined surface. The average MRR and the surface roughness obtained at different levels of process parameters are shown in Table 7. It is seen that high MRR is obtained at I_p- 9 A, T_{on} - 5 µs, T_{off}- 500 µs and low surface roughness is obtained at I_p- 6 A, T_{on} - 20 µs, T_{off}- 100 µs. Hence these are the optimum settings. Confirmation experiments were conducted at this setting which produced an average MRR of 38.15 mg/min and surface roughness of 3.21 µm. The maximum experimental error was 9.53 %.

Table 7 Average MRR and surface roughness.

	Material removal rate			Surface Roughness		
	I_p	T_{on}	T_{off}	I_p	T_{on}	T_{off}
1	15.98	27.69	19.85	4.90	7.76	5.87
2	19.76	22.16	24.81	6.80	6.88	6.94
3	28.46	14.35	19.55	9.95	7.01	8.85
Delta	12.48	13.34	5.26	5.05	0.88	2.98

CONCLUSION

In this study, electric discharge drilling of D2 steel is made using graphite electrode as tool. The effect of key parameters such as I_p, T_{on} and T_{off} on MRR and surface roughness of the machined surface is investigated, and following conclusions are drawn.

i. The MRR is significantly influenced by I_p (43.28 %), T_{on} (47.50 %) and the surfaces roughness is influenced by I_p (71.72 %) and T_{off} (25.08 %). The effect of T_{off} and T_{on} were marginal on MRR and R_a respectively.
ii. The process parameters are optimised to obtain high MRR (I_p- 9 A, T_{on} - 5 µs, T_{off} - 500 µs) and low surface roughness (I_p- 6 A, T_{on} - 20 µs, T_{off}- 100 µs). At

optimised settings the MRR and surfaces roughness is obtained is 38.16 mg/min and 3.39 µm respectively.

iii. The part of the vaporized metal solidifies in the form of spherical globules and its size become finer with increase in current.

Scope of the present work is limited to optimisation of settings to process parameters namely I_p, T_{on} and T_{off} on MRR and surface roughness while machining of D2 steel with graphite electrode. There is a need to explore the effect of these settings on electrode wear-rate and its pattern as well as combined optimisation of process parameters on MRR, R_a and EWR.

ACKNOWLEDGEMENT

This work is supported by Manipal Institute of Technology, Manipal Academy of Higher Education, Manipal, India.

REFERENCES

[1] Xavior MA, Adithan M. Determining the influence of cutting fluids on tool wear and surface roughness during turning of AISI 304 austenitic stainless steel, Journal of Materials Processing Technology, 2009; 209: 900–909

[2] Deepak D, Akash V, Winitthumkul N, Devineni Anjaiah. Machining of D2 heat treated steel using abrasive water jet: the effect of standoff distance and feed rate on kerf width and surface roughness, Journal of Research in Engg and Technology, 2014; 3(8): 417–421

[3] Vinothkumar S, Pradeepkumar M. Experimental investigation and optimization of machining process parameters in AISI D2 steel under conventional EDM and cryogenically cooled EDM process, Transactions of the Indian Institute of Metals, 2017; 70(9): 2293–2301.

[4] Pradhan MK, Biswas CK. Influence of process parameters on surface roughness in EDM of AISI D2 Steel: An RSM approach. International Conference Emerging Research in Advanced Mechanical Engineering, 2009; 1(9): 709–714.

[5] Nayak D, Sahu, SN, Mula S. Metallurgical approach towards explaining optimized EDM process parameters for better surface integrity of AISI D2 tool steel. Transactions of the Indian Institute of Metals, 2017; 70(5): 1183–1191.

[6] Klocke F, Schwade M, Klink A, Veselovac D. Analysis of material removal rate and electrode wear in sinking EDM roughing strategies using different graphite grades, Procedia CIRP, 2013; 6: 163–167.

[7] Al Hazza MHF, Khan AA, Ali MY, Hasim SF, Daud MRC. Study on capabilities of different electrode materials during EDM, IIUM Engineering Journal, 2017; 18(2): 189–195.

[8] Giandomenico N, Gorgerat FH, Lavazais B. Development of a new generator for die sinking electrical discharge machining, Procedia CIRP, 2016; 42: 721–726.

[9] Klocke F, Holsten M, Klink A. Technological and economic investigations on the application of metal infiltrated graphite electrodes for the sinking EDM of cemented carbides. Procedia CIRP, 2016; 42: 632–637.

[10] Lee CS, Heo EY, Kim JM, Choi IH, Kim DW. Electrode wear estimation model for EDM drilling, Robotics and Computer-Integrated Manufacturing, 2015; 36: 70–75.

[11] Izwan NSLB, Feng Z, Patel JB, Hung WN. Prediction of material removal rate in die-sinking EDM, Procedia Manufacturing, 2016; 5: 658–668.
[12] Sharif S, Safiei W, Mansor AF, Isa MHM, Saad RM. Experimental study of electrical discharge machine (die sinking) on stainless steel 316L using design of experiment, Procedia Manufacturing, 2015; 2 (2): 147–152.
[13] Doreswamy D, Javeri J. Effect of process parameters in electric discharge machining of D2 steel and estimation of coefficient for predicting surface roughness, International Journal of Machining and Machinability of Materials, 2018; 20(2): 101-117
[14] Kuppan P, Narayanan S, Oyyaravelu R, Balan AS. Performance evaluation of electrode materials in electric discharge deep hole drilling of Inconel 718 super alloy, Procedia engineering, 2017; 174: 53–59.
[15] Ablyaz TR, Shlykov ES, Kremlev SS. Copper-coated electrodes for electrical discharge machining of 38X2H2MA steel. Russian Engineering Research, 2017; 37(10): 910–911.
[16] Özerkan HB, Effect of changing polarity of graphite tool/ Hadfield steel workpiece couple on machining performances in die sinking EDM, MATEC Web of Conference, 2017; 129: 1–4.
[17] He L, Yu J, Duan W, Liu Z, Yin S, Luo H. Copper–tungsten electrode wear process and carbon layer characterization in electrical discharge machining. International Journal of Advanced Manufacturing Technology, 2016; 85(5-8): 1759–1768.
[18] Surtronic- 3 plus hand book. Retrieved from https://www.taylor-hobson.com/-/media/ametektaylorhobson/files/learning%20zone/user%20guides/surtronic%203-plus%20handbook.pdf?la=en; 19 November 2018.
[19] Ozgedik A, Cogun C. An experimental investigation of tool wear in electric discharge machining. International Journal of Advanced Manufacturing Technology, 2006; 27: 488-500.
[20] Bulent E, Erman A, Abdulkadir E. A semi-empirical approach for residual stresses in electric discharge machining. International Journal of Machine Tool & Manufacture, 2006; 46: 858-865.
[21] Marafona J, Chousal G. A finite element model of EDM based on the Joule effect. International Journal of Machine Tool & Manufacture, 2006; 46: 595-602.
[22] Ahsan Ali Khan. Role of heat transfer on process characteristics during electrical discharge machining. In: Bernardes MADS, editor. Developments in Heat Transfer, Rijeka: InTech, 2011, p 417-436.